Available online at www.sciencedirect.com

ScienceDirect

Biochimica et Biophysica Acta 1768 (2007) 1154–1159

Biochimica et Biophysica Acta BBA

www.elsevier.com/locate/bbamem

Expression and functionality of the Na^+/*myo*-inositol cotransporter SMIT2 in rabbit kidney

Karim Lahjouji [a], Rym Aouameur [a], Pierre Bissonnette [a], Michael J. Coady [a], Daniel G. Bichet [a,c], Jean-Yves Lapointe [a,b,*]

[a] *Groupe d'Étude des Protéines Membranaires (GÉPROM), département de Physiologie, Université de Montréal, Montréal, Québec, Canada H3T 1J4*

[b] *Département de Physique, Université de Montréal, Montréal, Québec, Canada H3T 1J4*

[c] *Centre de recherche Hôpital du Sacré-Coeur de Montréal 5400, boul. Gouin Ouest, Montréal, Québec, Canada H4J 1C5*

Received 15 September 2006; received in revised form 14 December 2006; accepted 10 January 2007
Available online 19 January 2007

Abstract

Myo-inositol (MI) is involved in several important aspects of cell physiology including cell signaling and the control of intracellular osmolarity i.e. by serving as a "compatible osmolyte". Currently, three MI cotransporters have been identified: two are Na^+-dependent (SMIT1 and SMIT2) and one is H^+-dependent (HMIT) and predominantly expressed in the brain. The goal of this study was to characterize the expression of SMIT2 in rabbit kidney and to compare it to SMIT1. First, we quantified mRNA levels for both transporters using quantitative real-time PCR and found that SMIT1 was predominantly expressed in the medulla while SMIT2 was mainly in the cortex. This distribution of SMIT2 was confirmed on Western blots where an antibody raised against a SMIT2 epitope specifically detected a 75 kDa protein in both tissues. Characterization of MI transport in brush-border membrane vesicles (BBMV), in the presence of D-*chiro*-inositol and L-fucose to separately identify SMIT1 and SMIT2 activities, showed that only SMIT2 is expressed at the luminal side of proximal convoluted tubules. We thus conclude that, in the rabbit kidney, SMIT2 is predominantly expressed in the cortex where it is probably responsible for the apical transport of MI into the proximal tubule.

Keywords: Myo-inositol transport; Membrane transport; SMIT2; Rabbit renal BBMV

1. Introduction

Myo-inositol (MI), a cyclic polyol, is the most biologically abundant stereo-isomer of the inositols which serve as precursors to molecules involved in cell signaling via the inositol phosphate pathways [1,2]. MI is also used as a "compatible osmolyte" allowing renal cells, amongst others, to function under hypertonic conditions [3]. The MI plasma concentration is approximately 50 μM and originates from both dietary intake and synthesis from glucose [4]. Its metabolism is highest within the kidney [3,5] where most of the MI transported at the apical membrane is oxidatively cleaved to yield D-glucuronic acid in proximal tubule cells. Cellular concentrations of MI can reach up to 30 mM, relying essentially on the activity of secondary active cotransporters [6]. To date, three MI transporters have been identified: two are Na^+-dependent, SMIT1 and SMIT2, while the third is H^+-dependent and is called HMIT.

SMIT1 was first isolated from Madin–Darby canine kidney (MDCK) cells using expression cloning in *Xenopus* oocytes [7]. In rats, mRNA encoding this transporter has been detected in kidney medulla, cortex, and brain using Northern blot analysis [7]. *In situ* hybridization showed that SMIT1 is predominantly present in the medullary and cortical thick ascending limb (TAL) and, to a lesser extent, in the inner medullary-collecting duct (IMCD) [8]. Mice in which SMIT1 was genetically removed demonstrated the critical importance of MI transporter during development as the mice died soon after birth due to respiratory failure, although neonatal lethality could be prevented by prenatal maternal MI supplement [9,10]. Altered transport and metabolism of MI are associated with several pathological conditions including Down's syndrome, Alzheimer's disease

* Corresponding author. Groupe d'Étude des Protéines Membranaires (GÉPROM), Université de Montréal, C.P. 6128, Succ. Centre-Ville, Montréal, Québec, Canada H3C 3J7. Tel.: +1 514 343 6111x7046; fax: +1 514 343 7146.
E-mail address: jean-yves.lapointe@umontreal.ca (J.-Y. Lapointe).

0005-2736/$ - see front matter © 2007 Elsevier B.V. All rights reserved.
doi:10.1016/j.bbamem.2007.01.007

[11] and several psychiatric disorders such as panic disorders, obsessive compulsive disorder and manic depression, for which clinical trials based on inositol treatments are being pursued.

A second Na^+-MI transporter, SMIT2, has an apparent Km of 120 μM based on measurements in oocytes expressing the protein [12]. In human tissues, SMIT2 was shown to be highly expressed in kidney, heart, skeletal muscle, liver and placenta with weak expression in the brain [13] while in rabbit, Hitomi and Tsukagoshi [14] showed that rat SMIT2 is expressed only in kidney and brain. SMIT2 transports D-*chiro*-inositol (DCI) equally well as MI but does not transport L-fucose, while SMIT1 transports L-fucose but not DCI [12,15]. When heterologously expressed in the MDCK renal cell line, SMIT2 is clearly targeted to the apical domain [16]. The third MI transporter, HMIT, is H^+-dependent and is predominantly expressed in the brain but very weakly elsewhere [17,18].

Only one study of MI transport in renal BBM has been published, more than 25 years ago [19] and it concluded that MI is transported *via* a sodium-coupled transporter. Transport was characterized with an apparent Km of 94 μM and the uptake was inhibited by D-glucose. No functional assessment of individual MI cotransporters in kidney has yet been published.

The goal of the present study is to characterize the expression of SMIT2 in rabbit kidney and to compare it to SMIT1. We show that SMIT1 is predominantly found in the renal medulla whereas SMIT2 is present in much greater amount in renal cortex. Analysis showed that SMIT2 is present both in kidney cortex and medulla, and is specifically enriched in BBMV. Functionality studies using purified BBMV extend earlier work and establish that SMIT2 is responsible for MI transport through the apical membrane.

2. Materials and methods

2.1. Materials

Radiolabelled ^{3}H-*myo*-inositol was purchased from Perkin Elmer (Boston, MA, USA) and nitrocellulose filters for uptake assays were from Millipore (Billerica, MA, USA). Trizol reagent and DNA primers for quantitative real time PCR (q-RT-PCR) were purchased from Invitrogen (Carlsbad, CA, USA) and PNGase F enzyme was obtained from New England BioLabs (Ipswich, MA, USA). Routine biochemicals were purchased either from Fisher Scientific (Ottawa, ON, Canada) or Sigma (Oakville, ON, Canada). Rabbits (New Zealand white male) weighing about 2 kg were provided by Charles River's Laboratories (St-Constant, QC, Canada). All animal experimentations were performed in accordance with the Canadian guidelines and with the Ethics Committee of the Université de Montréal.

2.2. Kidney Brush-border membrane vesicles isolation and MI transport procedure

Rabbit kidneys were excised, the capsules were removed and the outer cortex manually separated from the medulla using a scalpel. Brush border membrane vesicles (BBMV) were prepared using the magnesium precipitation technique [16] from fresh renal cortex only, since preparations made from frozen tissue exhibited a significantly decreased rate of MI transport. The intravesicular composition was 400 mM mannitol, 0.1 mM MgSO4, 50 mM HEPES–Tris, pH 7. BBMV were either used immediately or frozen in liquid nitrogen until use. Transport media (150 mM NaCl, 100 mM mannitol or L-fucose, 0.1 mM MgSO4 and 50 mM HEPES–Tris pH 7) contained tracer quantities of ^{3}H MI (specific activity 685 GBq/mmol) along with 50 nM cold substrate, unless otherwise specified in legends. L-fucose DCI, and alpha-methyl-D-glucose (αMG) were added to the transport media as equimolar replacements for mannitol. Transport of ^{3}H *myo*-inositol by renal BBMV was initiated by the addition of 50 μl BBMV to 950 μl transport medium at room temperature and, at given times, aliquots of 100 μl were filtered onto 0.65 μm nitrocellulose filters and immediately rinsed with 5 ml ice-cold substrate-free transport media. Filters were dissolved in scintillation cocktail (BetaBlend, ICN Biochemicals Inc., CA, USA) and tritium activity measured using a Beckman LS6000SC scintillation counter.

2.3. Quantitative-real-time PCR

Quantification of both SMIT1 and SMIT2 mRNA was performed using LUX technology along with the SuperScript™ III Platinum® one-step qRT-PCR System kit (Invitrogen). Total RNA was isolated from rabbit renal cortex and medulla using Trizol reagent (Life Technologies, Invitrogen). Primers and probes were designed using Primer software for LUX technology (https://orf.invitrogen.com/lux/). Quantifications were performed on 0.5 μg total RNA samples using the DNA Engine Opticon 2 PCR apparatus (MJ Research Inc, Walthman, MA, USA). Standards consisted of pure *in vitro* transcribed mRNA for either SMIT1 or SMIT2. The qRT-PCR protocol was: 50 °C (30 min) for reverse transcription, then 95 °C (2 min) followed by 50 cycles at 95 °C (15 sec) and 59 °C (30 sec). All reactions were run in triplicates and the quality of the PCR procedure monitored through melting curve analysis. The abundance of the target mRNAs was calculated according to a standard mRNA curve for both SMIT1 and SMIT2. Since the rabbit SMIT1 sequence is still unknown, primer's sequences were chosen from conserved regions in the SMIT1 sequences from other known species (rat, human and mouse). Primers used for SMIT1 were: CGG CTG AGT GGA TAC TTC CTG GCG (forward) and TCA CAA ACA GAG AGG CAC CAA T (reverse). For SMIT2, the primers sequences used were: CGC CGA CTG CTG AAT AAA GAT GGG (forward) and ATC ACC CTG GCC GTC CTC TAC (reverse).

2.4. Antibody production and Western blots

An anti-SMIT2 antibody was raised in rabbits (Biotechnology Research Institute, Montreal, QC, Canada; http://www.irb.cnrc.gc.ca) against a conserved amino acid sequence from the SMIT2 protein of rabbit, rat and human aligned using ClustalW software. The epitope contained 16 amino acid residues (FLALASNRSENSSCGL; amino acids 238 to 253 localized in the predicted intracellular loop between the predicted fifth and the sixth transmembrane domains. Care was taken to avoid sequence regions containing significant similarities to sequences of related transporters such as SMIT1 or to any SGLT sequences. The crude serum was tested on rabbit renal cortex, medulla and purified BBMV. The pre-immune serum was used as a negative control, and the specificity of the crude serum checked by peptide displacement assay.

Western blots were performed as described [16]. Briefly, samples were electrophoresed on a 7.5% polyacrylamide gel and transferred onto nitrocellulose membranes. The efficiency of the overall procedure was monitored by Ponceau red staining. The membranes were blocked with 5% non-fat milk in TBS-T (TBS+Tween 20, 0.1%), probed with the specific antibody at 1/500 dilution followed by probing with an HRP-linked goat anti-rabbit secondary antibody (Santa Cruz Biotech, CA) at 1/5000 dilution. All incubations with antibodies were performed in TBS-T with milk. Membranes were rinsed adequately between every step with TBS-T and revealed using enhanced chemiluminescence detection (Super-Signal®, Pierce, Canada).

2.5. PNGase assay

N-glycosylation was assayed using the PNGase F enzyme. Rabbit renal BBMV were subjected to PNGase treatment according to the manufacturer's procedure. The reaction mix was incubated for 3 h (or overnight) and proteins analyzed by Western blot as described above.

2.6. Statistical analysis

Values shown for transport studies represent means ± SE of triplicates and are expressed in nanomoles per mg protein. Protein content was determined using

the BCA assay (Pierce). Determination of kinetic parameters of MI transport was performed by fitting data to the Michaelis–Menten equation containing a non-specific component of uptake using Origin 6.1 software (OriginLab Corp., Northampton, MA, USA). Evaluation of the Ki value for DCI was performed using a competitive inhibition equation containing a non-specific component of uptake [20], also using Origin software. All uptake experiments, quantitative real-time PCR and Western blot analysis were performed on at least three separate occasions with comparable results. Data presented are from representative sets of experiments.

3. Results

3.1. Quantitative real-time PCR

In a first attempt to evaluate the relative levels of both SMIT1 and SMIT2, we quantified specific mRNA levels through qRT-PCR for both transporters SMIT1 and SMIT2 in total RNA extracted from renal cortex and medulla. As shown in Fig. 1, SMIT1 is predominantly found in the medulla ($2.9\pm 0.7\times10^3$ copies/μg total RNA vs. $0.8\pm0.04\times10^3$ copies/μg total RNA in cortex) whereas SMIT2 is present in greater amounts in cortex ($5.1\pm0.8\times10^3$ copies/μg total RNA vs. $0.8\pm 0.2\times10^3$ copies/μg total RNA) than in medulla.

3.2. Western blot analysis

In order to establish the renal distribution of SMIT1 and SMIT2 at the protein level, tissues from cortex and from medulla were studied using specific antibodies against SMIT2. In rabbit kidney tissues (Fig. 2), the antibody reveals a specific 75 kDa band in both cortex and medulla, one which appears to be highly enriched in BBMV. As shown in Fig. 2, we noticed that fainter bands with reduced molecular weight (MW) can occasionally be observed. This presumably represents some degradation products of SMIT2. As shown in this figure, all of the specific signals seen in the presence of the anti-SMIT2 antibody (immune) are absent when treated with the pre-immune serum fraction and are displaced by peptide preadsorption of antibody. PNGase F treatment was also performed in order to test the possibility that the 75 kDa protein is a glycosylated protein. As seen in Fig. 2, assays performed on purified BBMV show no reduction of MW, indicating that SMIT2 is not N-glycosylated in these tissues. Even after 16 h incubation in the presence of PNGase F, no alterations in MW were detected (not shown).

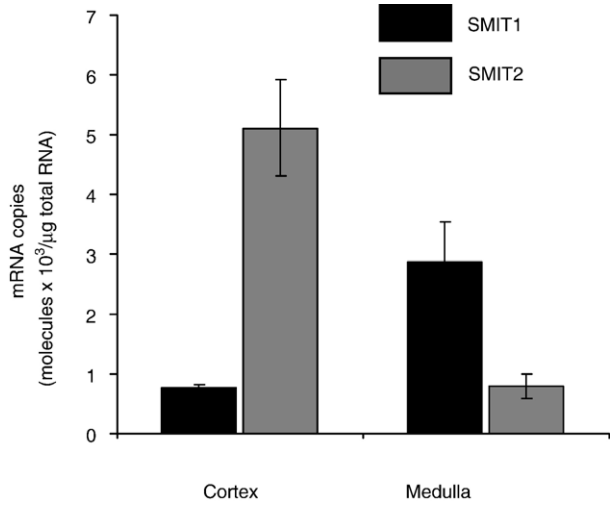

Fig. 1. Quantitative RT-PCR (qRT-PCR) determination of mRNA for SMIT1 and SMIT2 transporters. qRT-PCR was performed using primers that are specific for SMIT1 or SMIT2 (see Materials and methods) using 0.5 μg total RNA as template. Absolute quantification (molecules/μg total RNA) is made possible by interpolation of standard curves for both mRNA using pure cRNA for both species. Bars are mean±SEM from three independent experiments, each performed in triplicates.

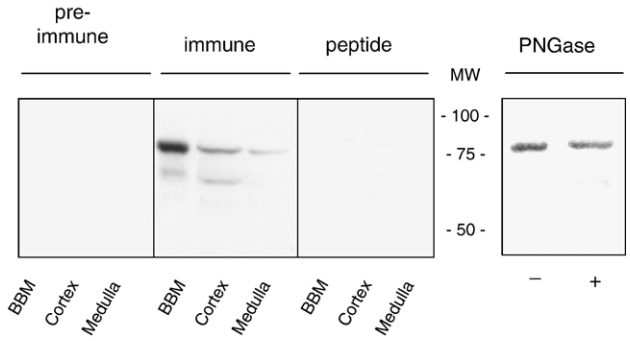

Fig. 2. Identification of SMIT2 protein in rabbit renal tissues using Western blot detection. SDS-PAGE and transfer on nitrocellulose were performed as described in Materials and methods. Membranes were blotted either against pre-immune sera or against anti-SMIT2 antibody (both at 1/500) either with (peptide) or without (immune) pre-adsorption to specific SMIT2 peptide on rabbit tissues: purified rabbit brush-border membrane vesicles (BBMV) (lane 1, 2 μg protein per lane), kidney homogenates (100 μg per lane) from cortex (lane 2) or medulla (lane 3). A 75-kDa specific band is detected. The right hand panel shows the evaluation of SMIT2 N-glycosylation in purified BBMV. Homogenates (2 μg protein per lane) were treated (+) or not (−) with PNGase for 3 h prior Western blot analysis. In both cases, a similar 75 kDa protein is detected.

3.3. MI transport in purified BBMV

Although an MI transport system(s) in renal BBMV has already been reported [16], the molecular identity of the transporter(s) involved has not yet been determined. The activity of SMIT1 can be distinguished from the activity of SMIT2 by using L-fucose which is specifically transported by SMIT1 and DCI which is specifically transported by SMIT2. Fig. 3 illustrates the uptake of ^{3}H-MI (in the presence of 50 nM unlabelled MI) into renal BBMV as a function of time, either alone or in the presence of a saturating concentration of either DCI (1 mM) or L-fucose (100 mM) to selectively inhibit SMIT2 and SMIT1 respectively, or in the presence of saturating unlabelled MI to inhibit all MI-specific transport systems. Total MI transport (●) displayed linearity for 2–3 min and the uptake curve demonstrates a typical overshoot indicative of secondary active transport systems (Na^+ dependent, in this case). In the presence of 100 mM L-fucose (■), the specific rate of radiolabelled MI transport is reduced by 35% while in presence of a saturating concentration of MI (△), the uptake is reduced to 80%. When the transport assay is performed in the presence of 1 mM DCI (▲), MI uptake is also reduced by 80%.

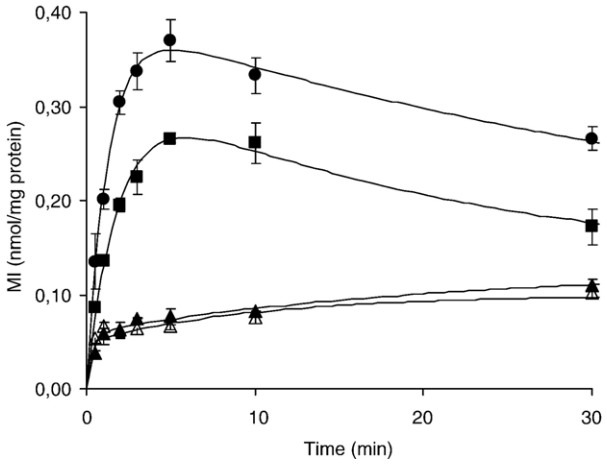

Fig. 3. Time course of MI transport into rabbit BBMV. Rabbit BBMV (50 μl) were incubated with 950 μl transport media containing 50 nM MI along tracer (see Materials and methods for composition of transport media). Uptakes were performed either in absence (●) or presence of saturating L-fucose (100 mM, ■), MI (1 mM, △) or DCI (1 mM, ▲). Addition of L-fucose was performed in equimolar replacement with mannitol. Aliquots of 100 μl were taken for each sample. Data are mean±SEM of triplicates. When not shown, error bars are smaller than symbol.

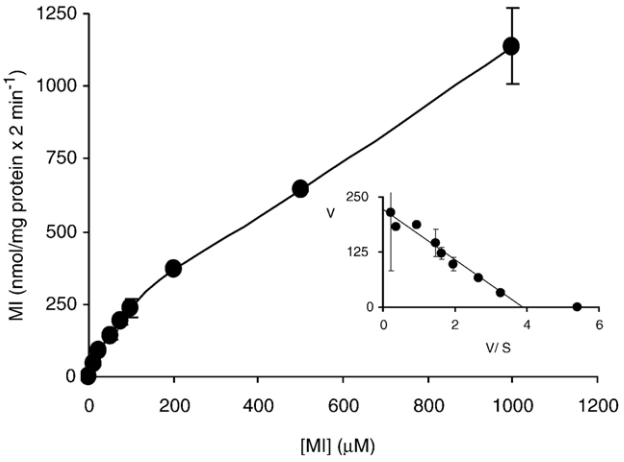

Fig. 5. Determination of kinetic parameters for MI transport in renal rabbit BBMV. 2 min uptakes were performed with increasing concentrations of MI (up to 1 mM). Aliquots of 100 μl were taken for each sample. Data are mean± SEM of triplicates. When not shown, error bars are smaller than symbol. Inset presents Eadie–Hofstee transformation of total uptake to which was subtracted non-specific fraction (Kd component). Kinetic parameters determined were 221±26 nmol×mg protein^{-1}×2 min^{-1} for Vmax, 57±14 μM for Km and 0.92±0.03 nmol/mg protein^{-1}×2 min^{-1} for the non-specific Kd value.

Since DCI and L-fucose inhibitions should be complementary with respect to the overall profile of MI transport, the partial inhibition induced by L-fucose was somewhat inconsistent with the similar uptake levels seen in the presence of DCI and MI. We thus further investigated the inhibitory profile of MI transport on BBMV by using increasing concentrations of L-fucose, DCI or MI. As shown in Fig. 4, both MI and DCI induced a considerable inhibition of radiolabelled MI uptake with comparable efficiencies. On the other hand, L-fucose still only partially impeded the uptake of MI (38% reduction at 100 mM). This inhibition was however incompatible with a competitive effect displaying a Ki of 4.7±1.0 mM as is seen with MDCK cells [16]. L-*chiro*-inositol (LCI, 1 mM), a non-inhibitory stereo-isomer of DCI, showed no significant inhibition of MI transport, as α-methyl-glucose (αMG, 1 mM), specific substrate of the Na^+/glucose transporter SGLT1. This indicates that these compounds do not interfere with the BBMV MI transport.

Fig. 5 shows a typical example of MI transport measurements at different MI concentrations, performed in the absence of L-fucose. The data were analysed with an equation representing a single site+passive diffusion. The kinetic parameters determined for the saturable component were 57±14 μM for Km and 221±24 nmol/mg protein^{-1}×2 min^{-1} for Vmax. Transposition of the saturable portion of the uptake experiment as Eadie–

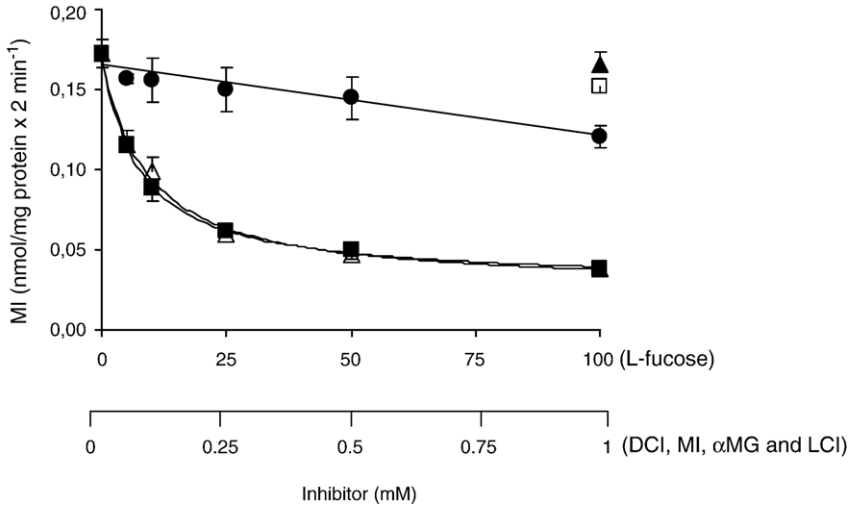

Fig. 4. Initial rate of MI transport in absence or presence of potential inhibitors, α-methyl-glucose or L-fucose, DCI, LCI, or MI. Inhibition studies of initial rate uptakes (2 min) of 50 nM MI by various effectors on rabbit BBMV were performed as described in this figure and Materials and methods. Inhibitors used were αMG (10 mM, ▲), DCI (up to 1 mM, △), L-*chiro*-inositol (1 mM, □), L-fucose (up to 100 mM, ●) and MI (up to 1 mM, ■). Data are mean±SEM of triplicates. When not shown, error bars are smaller than symbol.

Hofstee plot is shown in the inset. By using these kinetic parameters and equation for competitive inhibition [21], we were able to determine a Ki value of 63 ± 17 μM for DCI inhibition of MI uptake for the data presented in Fig. 4.

4. Discussion

To date, three MI transport systems have been identified; SMIT1, SMIT2 and HMIT, but their individual physiological functions have not yet been well delineated. For this reason, this study aimed to examine the relative contributions of SMIT1 and SMIT2 to MI transport in the rabbit kidney. Although HMIT was shown to be weakly expressed in the rat kidney, its involvement in MI transport through rabbit renal BBMV can be ruled out since the uptake observed is totally Na^+-dependent [19] while HMIT transports MI in a H^+-dependent manner and is largely inefficient at neutral pH levels (≥ 7.0) [17,18]. In the present study, using qRT-PCR evaluation, we demonstrated the presence of both SMIT1 and SMIT2 in rabbit kidney, and found that they exist in different proportions in cortex vs. medulla. These are the first quantitative data concerning renal expression of the SMIT proteins and they are in agreement with Northern blot analysis previously published for rabbit SMIT2 [14] which determined that SMIT2 is expressed only in the brain and the kidney, although the latter was not further investigated for cortex and medulla subdistribution. In human, also using Northern blot, Roll et al. [13] have found a broader distribution for SMIT2 expression including heart, skeletal muscle, kidney, liver, and placenta while weaker expressions were found in brain and several other tissues. We do not know if the differences between these results are due to species differences or to methodology. Unfortunately, these discrepancies were not discussed in the study [13]. Quantization of mRNA through qRT-PRC represents an advantage over Northern blots in terms of evaluating mRNA distribution in tissues. Data on SMIT1 and SMIT2 evaluation by qRT-PCR have not yet been reported for other species. The fact that SMIT1 and SMIT2 have different distributions within the kidney, SMIT1 being more abundant in medulla while SMIT2 mainly being expressed in cortex, suggests tissue-specific functions for each transporter. A major difference between these two transporters is their polarized location within epithelial cells, since SMIT1 is usually detected at the basolateral membrane while SMIT2 is rather found at the apical domain of these cells [16]. In a previous report from our laboratory [16], the characterization of MI transport in BBMV has shown that the presence of 100 mM L-fucose inhibits MI transport by about 30% suggesting the presence of some SMIT1 at this membrane. In the present study, we have performed a more complete inhibition study using both L-fucose, a specific inhibitor of SMIT1, and DCI which specifically inhibits SMIT2 in order to better distinguish the two systems. The results obtained (Fig. 4) confirmed the partial effect of L-fucose previously reported but appear to be inconsistent with the total effect of DCI. Indeed, the partial inhibition by L-fucose suggests the presence of both SMIT1 and SMIT2 while the complete inhibition achieved with DCI, clearly indicates that only SMIT2 is found in rabbit BBMV. Unfortunately, no anti-SMIT1 antibodies are presently available to allow a direct detection of SMIT1 by Western blot or immunofluorescence. Still, while 1 mM DCI is sufficient to attain complete MI transport inhibition, 100 mM L-fucose is necessary to induce partial inhibition, one that has not even reached statistical significance at 50 mM. Such a linear inhibition profile is incompatible with the L-fucose-mediated inhibition of SMIT1 in normal MDCK cells, for which a Ki value of 4.8 ± 1.0 mM was observed [16]. Instead, the large concentrations of L-fucose may reduce MI transport indirectly through an effect on the Na^+ electrochemical gradient. The linear Eadie–Hofstee plot displayed in the insert of Fig. 5, showing a Km value compatible with that found by Hammerman et al. [19], cannot be used to rule out the presence of a second transport site since both SMIT1 and SMIT2 share similar Km values. A possible contribution of the Na^+/glucose cotransporter SGLT1 to MI transport in BBMV was ruled out by evaluation of MI uptake in the presence of a saturating concentration of a substrate for SGLT1 (αMG) which is not recognized by either SMIT1 nor SMIT2 [12,22]. We thus conclude that the effect of 100 mM L-fucose on MI transport is indirect and that SMIT2 is the only MI transport system in the apical membrane of the proximal convoluted tubule cells as shown by the complete inhibition of MI uptake by DCI. This conclusion would suggest a cellular model where SMIT1 and SMIT2 are restricted to the basolateral and apical membranes, respectively.

In addition to the first anti-SMIT2 antibody previously used in our laboratory [16], a second SMIT2-specific antibody was raised, this time against a new epitope. This antibody, used throughout the present work, recognizes in kidney tissues a 75 kDa band which closely corresponds to the expected MW for this protein according to the deduced amino acid sequence (≈ 74 kDa). The faint lower MW bands seen in all lanes of Fig. 2 are most probably degradations of this protein and are not believed to represent specific variants of SMIT2. This 75 kDa band was found to be more abundant in renal cortex (lane 2) than in renal medulla (lane 3) and was further enriched in purified BBMV (lane 1). This is in accordance with the data obtained by qRT-PCR from the same tissues. In all cases, both these bands were found to be specific as they are absent when detected with pre-immune serum and are displaced by preadsorption of antibody with peptide. Since SMIT2 possesses an N-glycosylation motif, the possibility that the 75 kDa is a glycosylated form of the protein was investigated. As shown in Fig. 2, PNGase F treatment performed on BBMV showed no reduction of MW when compared to controls. It should be noted that PNGase assays were also prolonged for up to 16 h in order to confirm this finding. The absence of glycosylation is not surprising since proteins which do not contain a signal peptide, as is the case for SMIT2, are less incline to acquire such residues even though they have adequate N-glycosylation motif. Also, it is worth mentioning that the specific 75 kDa band was also evidenced in other rabbit tissues such as brain and lung (not shown).

Although the glucose content (5.5 mM) in ultrafiltrate is much higher than that of MI (50 μM), the affinity of SMIT2 for glucose is remarkably lower (≈40 mM, [12]) than that for MI (57 μM). Physiologically, under such conditions where the MI concentration is equivalent to its Kt while the concentration of glucose is eight times lower than its Kt, MI would be the predominant substrate for the transporter. Furthermore, since glucose is efficiently reabsorbed through SGLT proteins along the proximal tubule, the substrate competition for SMIT2 will rapidly drop in favour of MI. For these reasons, we believe that glucose represents only a small hindrance to MI uptake through SMIT2 along the proximal tubule.

In conclusion, our results reveal that the rabbit kidney expresses both SMIT1 and SMIT2, but in opposing proportions in cortex and medulla. SMIT2 is predominantly expressed in the cortex where it probably serves as the unique MI transporter across the apical membrane of the proximal tubule. On the other hand, SMIT2 is also expressed, albeit at a lower level in the medulla but its specific role remains to be elucidated.

Acknowledgment

This work was supported by the Canadian Institutes of Health Research (CIHR), grant #MOP-67038.

References

[1] C.P. Downes, C.H. Macphee, myo-inositol metabolites as cellular signals, Eur. J. Biochem. 193 (1990) 1–18.
[2] S.K. Fisher, J.E. Novak, B.W. Agranoff, Inositol and higher inositol phosphates in neural tissues: homeostasis, metabolism and functional significance, J. Neurochem. 82 (2002) 736–754.
[3] M.B. Burg, Renal osmoregulatory transport of compatible organic osmolytes, Curr. Opin. Nephrol. Hypertens. 6 (1997) 430–433.
[4] F.X. Beck, A. Burger-Kentischer, E. Muller, Cellular response to osmotic stress in the renal medulla, Pflugers Arch. 436 (1998) 814–827.
[5] J.S. Handler, H.M. Kwon, Regulation of the myo-inositol and betaine cotransporters by tonicity, Kidney Int. 49 (1996) 1682–1683.
[6] R. Dolhofer, O.H. Wieland, Enzymatic assay of myo-inositol in serum, J. Clin. Chem. Clin. Biochem. 25 (1987) 733–736.
[7] H.M. Kwon, A. Yamauchi, S. Uchida, A.S. Preston, A. Garcia-Perez, M.B. Burg, J.S. Handler, Cloning of the cDNa for a Na+/myo-inositol cotransporter, a hypertonicity stress protein, J. Biol. Chem. 267 (1992) 6297–6301.
[8] A. Yamauchi, A. Miyai, S. Shimada, Y. Minami, M. Tohyama, E. Imai, T. Kamada, N. Ueda, Localization and rapid regulation of Na+/myo-inositol cotransporter in rat kidney, J. Clin. Invest. 96 (1995) 1195–1201.
[9] G.T. Berry, S. Wu, R. Buccafusca, J. Ren, L.W. Gonzales, P.L. Ballard, J.A. Golden, M.J. Stevens, J.J. Greer, Loss of murine Na+/myo-inositol cotransporter leads to brain myo-inositol depletion and central apnea, J. Biol. Chem. 278 (2003) 18297–18302.
[10] J.F. Chau, M.K. Lee, J.W. Law, S.K. Chung, S.S. Chung, Sodium/myo-inositol cotransporter-1 is essential for the development and function of the peripheral nerves, FASEB J. 19 (2005) 1887–1889.
[11] J.E. Nestler, D.J. Jakubowicz, P. Reamer, R.D. Gunn, G. Allan, Ovulatory and metabolic effects of D-*chiro*-inositol in the polycystic ovary syndrome, N. Engl. J. Med. 340 (1999) 1314–1320.
[12] M.J. Coady, B. Wallendorff, D.G. Gagnon, J.Y. Lapointe, Identification of a novel Na+/myo-inositol cotransporter, J. Biol. Chem. 277 (2002) 35219–35224.
[13] P. Roll, A. Massacrier, S. Pereira, A. Robaglia-Schlupp, P. Cau, P. Szepetowski, New human sodium/glucose cotransporter gene (KST1): identification, characterization, and mutation analysis in ICCA (infantile convulsions and choreoathetosis) and BFIC (benign familial infantile convulsions) families, Gene 285 (2002) 141–148.
[14] K. Hitomi, N. Tsukagoshi, cDNA sequence for rkST1, a novel member of the sodium ion-dependent glucose cotransporter family, Biochim. Biophys. Acta 1190 (1994) 469–472.
[15] R.E. Ostlund Jr., R. Seemayer, S. Gupta, R. Kimmel, E.L. Ostlund, W.R. Sherman, A stereospecific myo-inositol/D-*chiro*-inositol transporter in HepG2 liver cells. Identification with D-*chiro*-[3-3H]inositol, J. Biol. Chem. 271 (1996) 10073–10078.
[16] P. Bissonnette, M.J. Coady, J.Y. Lapointe, Expression of the sodium-myo-inositol cotransporter SMIT2 at the apical membrane of Madin–Darby canine kidney cells, J. Physiol. 558 (2004) 759–768.
[17] M. Uldry, M. Ibberson, J.D. Horisberger, J.Y. Chatton, B.M. Riederer, B. Thorens, Identification of a mammalian H(+)-myo-inositol symporter expressed predominantly in the brain, EMBO J. 20 (2001) 4467–4477.
[18] M. Uldry, P. Steiner, M.G. Zurich, P. Beguin, H. Hirling, W. Dolci, B. Thorens, Regulated exocytosis of an H+/myo-inositol symporter at synapses and growth cones, EMBO J. 23 (2004) 531–540.
[19] M.R. Hammerman, B. Sacktor, W.H. Daughaday, myo-Inositol transport in renal brush border vesicles and it inhibition by D-glucose, Am. J. Physiol. 239 (1980) F113–F120.
[20] P. Bissonnette, H. Gagne, M.J. Coady, K. Benabdallah, J.Y. Lapointe, A. Berteloot, Kinetic separation and characterization of three sugar transport modes in Caco-2 cells, Am. J. Physiol. 270 (1996) G833–G843.
[21] P. Bissonnette, J. Noel, M.J. Coady, J.Y. Lapointe, Functional expression of tagged human Na+-glucose cotransporter in *Xenopus laevis* oocytes, J. Physiol. 520 (Pt. 2) (1999) 359–371.
[22] K. Hager, A. Hazama, H.M. Kwon, D.D. Loo, J.S. Handler, E.M. Wright, Kinetics and specificity of the renal Na+/myo-inositol cotransporter expressed in *Xenopus* oocytes, J. Membr. Biol. 143 (1995) 103–113.